



Bachelor Project

Christian Terkelsen Holme

Analysis of the isotopic composition of the NEGIS ice core including a comparison with coastal temperature data

De fysiske fag - geofysik

Academic advisor: Bo Mølløse Vinther

Co-advisor: Trevor James Popp

Submitted: 12/06/13

Abstract

This project deals with a water isotopic based examination of a 0-29 meter shallow firn core from the North East Greenland Ice Stream (NEGIS). The objective is to analyse the variability in the isotopic composition and compare it with recorded temperatures from different coastal stations around Greenland. During this project, the ice core was cut into 5 cm discrete samples, melted, and hereafter measured with a commercialised near-infrared cavity ringdown spectrometer to obtain δD and $\delta^{18}O$ values for each water sample with respect to VSMOW. Results show that a strong diffusion is dominating the seasonal signal of the isotopic composition, thus the seasonal signal is smoothed out after 10 meters. A dating of the core with a precision of 1 year is presented based on a combined analysis of the isotopic composition, Na^+ , NH_4^+ , SO_4^{2-} and dust. The accumulation rate is estimated to $11 \pm 2 \frac{cm}{y}$ (1877-2012), but the variability of annual precipitation does not correlate with the variability of $\delta^{18}O$, likely a result of topographic undulations and upstream effects. The $\delta^{18}O$ data and the recorded coastal temperatures were examined for correlations. The most significant correlation coefficient was obtained between Tasiilaq and the $\delta^{18}O$, where a coefficient of 0.189 was found. The deuterium excess has been found to have an anti-correlation of -0.170 with the averaged sea surface temperature (SST,0-70N), whereas $\delta^{18}O$ is found to have a weak correlation coefficient of 0.245 with SST. The low correlations are likely to be a consequence of the large distance between the coastal stations and the NEGIS site, sastrugi and strong diffusion dominating the isotopic composition.

Resumé

Dette projekt omhandler en analyse af den isotopiske sammensætning af isen fra en 0-29 meter firn kerne fra den Nordøstgrønlandske Is Strøm (NEGIS). Formålet er at analysere den årligt varierende isotopsammensætning, og sammenligne det med målte temperature fra forskellige kyststationer omkring Grønland. I dette projekt er firnkernen skåret i 5 cm diskrete prøver, der blev målt med en kommercialiseret near-infrared cavity ringdown spectrometer. Spektrometeret udregnede δD og $\delta^{18}O$ for de tilhørende prøver, og dette projekt kalibrerer dataene med hensyn til VSMOW. Resultaterne viser, at en stærk diffusion dominerer sæson-signalet af den isotopiske sammensætning, og at diffusionen udglatter det sæsonsvingende signal efter 10 meter. En datering af kernen med en præcision på 1 år er præsenteret, baseret på en samlet analyse af den isotopiske sammensætning, Na^+ , NH_4^+ , SO_4^{2-} og støv. Akkumulationsraten er estimeret til $11 \pm 2 \frac{cm}{y}$ (1877-2012), men den årligt varierende nedbør stemmer ikke overens med den årligt varierende $\delta^{18}O$, hvilket sandsynligvis er et resultat af topografiske undulationer og opstrømseffekter. $\delta^{18}O$ dataene og de målte kyst temperature var undersøgt for korrelering. Den mest signifikante korrelation koefficient fandtes mellem Tasiilaq og $\delta^{18}O$, hvor en koefficient på 0.189 fundet. Deuterium excess anti-korrelerer med den gennemsnitlige havoverflade temperatur (SST,0-70N), hvorimod $\delta^{18}O$ har en svag korrelations koefficient på 0.245 med SST. De lave korrelationer er sandsynligvis en konsekvens af den store afstand mellem kyststationerne og NEGIS sitet, sastrugi og den stærke diffusion som dominerer den isotopiske sammensætning.

Contents

Abstract	ii
1 Introduction	1
2 Theory	1
2.1 Stable isotopes	1
2.1.1 Stable isotopes in the ice	2
2.2 The ice core	3
2.2.1 The site	3
2.2.2 Dating of the ice core	3
2.3 Deuterium excess	4
2.4 Precipitation	5
3 Experiment	5
3.1 Sampling the ice core	5
3.2 IR cavity ringdown spectroscopy	6
3.2.1 Theory behind the spectroscopy	6
3.2.2 Procedure	7
4 Results	9
4.1 Data processing	9
4.2 Calibration	9
4.3 Error analysis	9
4.4 Data	10
5 Discussion	14
6 Conclusion	18
Bibliography	19

1 Introduction

The climate has always been of great interest to humankind. Particular in recent times has an increasing focus evolved, enhanced by global warming. However, what is possible to predict about the future? In understanding the future, it is essential to understand the past. The ice sheets on Greenland and Antarctica works as data banks with preserved climate proxy data from the past, hereby enabling the possibility of recording the past.

Every year snow accumulates on the ice sheets. Therefore, by drilling ice cores through the ice sheets, it is possible to determine the isotopic composition of past precipitation, which works as a representation of the climatic past. This is a result of the difference between heavy (H_2^{18}O and DHO) and light (H_2^{16}O) water isotopes being traceable from the evaporation site in the tropics all the way to the precipitation site - chapter 2.1.1. Based on this, it has been possible to classify the different ice ages, the varying temperature and amount of greenhouse gasses back in time. Basically, knowledge about the past is a strong tool in the search for understanding the future, because it reveals the climatic patterns, which is essential when analysing the future.

This project aims to analyse the upper 29 meters of The NEGIS (North East Greenland Ices-tream) ice core. In reality it is a firn core given its low density, however, I will use the names firn - and ice core loosely.

Technology such as laser spectroscopy makes it possible to determine the concentration of the different isotopes at a certain depth. In this project, a commercialised near-infrared cavity ringdown spectrometer from the manufacturer Picarro of brand L2120-i is used. However, high accumulation inhibits diffusion, and the low accumulation rate at this site produces increased diffusion and increased smoothing across annual layers, making it difficult to determine the age solely from the isotopic composition. As a result of this, density, volcanic eruptions and other seasonal varying parameters will be introduced with the purpose of clarifying the age. Based on the age-depth relationship and the measured stable isotopes, it is possible to analyse the relationship between the stable isotopes and the year of precipitation. It is then possible to compare the information about the annual accumulated snow and the recorded coastal stations around Greenland, to give an interpretation of the temperature change of the last hundred years.

2 Theory

2.1 Stable isotopes

An isotope is a variant of a given chemical element, where the amount of protons stay fixed and the neutrons can vary.

Water molecules have different isotopologues such as H_2^{16}O , H_2^{18}O and HD^{16}O , but the heavier isotopes such as H_2^{18}O [0.200%] and HD^{16}O [0.032%] are rare compared to the abundant H_2^{16}O [99.768%] (Mook, 2000) - the brackets define the relative abundance. The different isotopologues are a helpful tool, when examining ice cores, but first it is important to know the differences between them.

The ratio between abundant and rare isotopes is described by:

$$R = \frac{[\text{H}_2^{18}\text{O}]}{[\text{H}_2^{16}\text{O}]} \quad (2.1)$$

This ratio is compared to a standard ratio R_s (VSMOW - Vienna Standard Mean Ocean Water) and subtracted by 1 to find its deviation from unity (Cuffey and Paterson, 2010). Because of

the low values, multiplying by 1000 ‰ is useful:

$$\delta = \left(\frac{R - R_s}{R_s} \right) \cdot 1000\text{‰} = \left(\frac{R}{R_s} - 1 \right) \cdot 1000\text{‰}. \quad (2.2)$$

This δ -relationship is possible to determine as a consequence of the relationship between molecules' average kinetic energy and their temperature:

$$\frac{1}{2} \cdot m \cdot \bar{v}^2 = K \cdot T. \quad (2.3)$$

Here m is the mass of the molecule, \bar{v} is the mean diffusion velocity, K is Boltzmann's constant and T is the temperature. A result of equation 2.3, is that molecules have the same $1/2m\bar{v}^2$ regardless of the isotopic content. Hence, molecules with higher masses have lower diffusion velocities and vice versa (Mook, 2000).

In relation to quantum mechanics, the mass of a molecule determines its energy (Griffiths, 2004). First the frequency of vibration is given by:

$$\nu = \frac{1}{2\pi} \sqrt{\frac{k}{m}}, \quad (2.4)$$

Where k is the force constant for the water molecule, and h is the Planck constant. Furthermore, the vibrational energy is defined as:

$$E_{vib} = \frac{1}{2} \cdot h \cdot \nu. \quad (2.5)$$

Therefore, heavier isotopes will have lower vibrational energies, thus forming stronger bonds in the compound. This fact combined with the low diffusion velocity leads to lower collision frequencies for heavier isotopes, which explains why lighter isotopes react faster. As a consequence, heavier isotopes like H_2^{18}O and HD^{16}O have lower vapour pressure relative to the lighter and more abundant H_2^{16}O . A high vapour pressure leads to a higher tendency towards evaporation, which underlies the fractionation of water isotopes in natural systems (Cuffey and Paterson, 2010).

2.1.1 Stable isotopes in the ice

Willi Dansgaard discovered the relationship between the amount of heavy oxygen isotopes in precipitation and the temperature at the precipitation site (Dansgaard, 1954). When water evaporates in the subtropics it moves toward the poles. As a consequence of the heavy isotopes' low vapour pressure, they have lower tendency to evaporate from the ocean source than the lighter isotopes, while they condensate more easily to form precipitation (Cuffey and Paterson, 2010).

Furthermore, the Clausius-Claperoynt relationship states that the cooling of an air mass drives condensation and precipitation (Wallance and Hobbs, 2006). Thus, when an air mass travels to high latitudes, its corresponding delta-value will become lower and lower as the air mass loses heavy isotopes via precipitation. Basically, when the precipitation accumulates as snow on the ice sheet, it will be lighter than the reservoir from which it came.

This can be used to analyse the temperatures of the past by looking at the varying isotopic composition. In addition to that, if the temperature was low at the precipitation site, then the amount of heavy isotopes falling as snow on the ice sheet will be relatively low, whereas if it was warmer then the value of $\delta^{18}\text{O}$ would be higher. This isotopic composition is possible to measure if enough precipitation is provided (for clarification - see chapter 2.2.1), which illustrates a seasonal cycle that enables a dating of the ice core, and determination of temperatures.

2.2 The ice core

2.2.1 The site

The ice core used in this experiment originated from NEGIS (75.6N, 36.0W, elevation: 2542 m), and was drilled in the summer of 2012 - see figure 2.1 for location. Different areas of Greenland have different precipitation rates, surface temperatures, basal temperatures, etc. The NEGIS site has been exposed to quite a low precipitation rate, approximated to $11 \pm 2 \frac{\text{cm}}{\text{y}}$ from 1877-2012 (clarification is given in chapter "Precipitation"). Normally, there has to be a minimum of 20 cm ice per year in order to date an ice core using isotopes. With only around half that amount, dating the ice core becomes more complicated, and other techniques have been implemented.

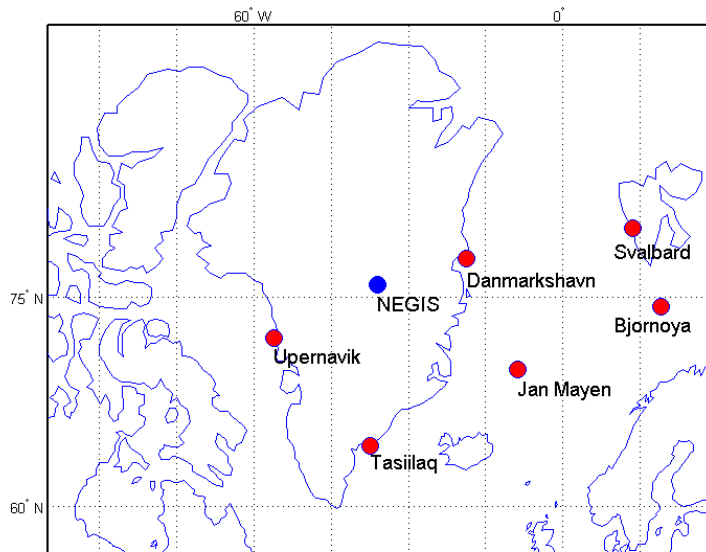


Figure 2.1: Map of Greenland, showing the locations mentioned in this report. The NEGIS site (blue dot) and the different coastal stations (red dots). The specific coordinates of the coastal stations are provided in table 4.2.

2.2.2 Dating of the ice core

A wide variety of features are relevant to examine when estimating the age down through the depth of the ice core. For layer counted chronologies, seasonal variability in ice properties or impurities can be used. For instance, it is possible to determine the isotopic composition of the ice core using the Continuous Flow Analysis (CFA), where every 55 cm of the ice core is melted and measured continuously (Gkinis et al., 2010), contrary to the discrete measurements, which is used as the temperature analysis in this project. The CFA is, however, primarily used to detect the impurities of the ice core, which include Na^+ , NH_4^+ , SO_4^{2-} and dust. These different impurities vary seasonally, which makes it possible to detect annual cycles in the ice core. In this project, a program developed by Sune Olander Rasmussen called Datetool2 is used (Rasmussen, 2006b). This program collects all the data correlated with depth, which makes it possible to match the seasonal variability for the different parameters and hereby determine the age down through the core. Figure 4.4 provides an example.

The combination of the different variables makes it possible to determine an overall annual cycle

down through the core based on the combined pattern in the data.

A year is marked in the winter, which happens every time Na^+ has its peak due to the strong winds during the fall. Na^+ is a result of the transport of salt from the ocean. Accordingly, the verification of the Na^+ peaks are possible by comparing with the seasonal variabilities of the remaining parameters. Dust peaks in the spring during interglacial periods such as the present as a result of storms (Cuffey and Paterson, 2010), whereas NH_4^+ has its peak in summer. In the case of NH_4^+ , some disagreement exists regarding whether or not it's caused by wildfires. However, regardless of its origin, a common agreement exists treating the property as a seasonal parameter (Rasmussen et al., 2006). SO_4^{2-} is an indicator of volcanic eruptions. Knowledge about past volcanic eruptions is a helpful tool when determining the age at a given depth with certainty. This is a result of the acid fallout (SO_4^{2-}) from the volcanic eruptions, which creates a strong acid signal. Comparing with historical data, it is possible to determine the precise date of the eruption at the given depth, which is very helpful when dating the ice core - see table 2.1. Table 2.1 shows the volcanic eruptions recorded in the upper 45 meters of the ice core. Although this project only focuses on the upper 29 meters, it is useful to look at the previous eruptions such as Laki. This gives a greater insight in the compression of the annual layers, which is used when determining the annual mean precipitation at the site.

Volcano	Katmai	Krakatoa	Tambora	Laki
Year A.D.	1912	1885	1816	1783
Depth [m]	22.8	27.3	39.1	44.3

Table 2.1: Year and depth for the volcanic eruptions detected in the NEGIS core. This project focuses on the upper 29 meter.

2.3 Deuterium excess

The δD and $\delta^{18}\text{O}$ values for the same sample have been shown to lie close to a straight line:

$$\delta\text{D} = 8 \cdot \delta^{18}\text{O} + 10\text{‰}. \quad (2.6)$$

This is called the global meteoric water line, (Craig, 1961). The equation consists of 8 times $\delta^{18}\text{O}$ caused by the relative mass difference between D and ^1H , which is 8 times higher than the difference between ^{18}O and ^{16}O . This is a consequence of the amount of abundant and rare isotopes for the different molecules.

Willi Dansgaard was the first to define deuterium excess, or a water sample's deviation from the global meteoric water line (Dansgaard, 1964).

$$d = \delta\text{D} - 8 \cdot \delta^{18}\text{O}. \quad (2.7)$$

Deuterium excess is affected by the ocean temperature, which, due to its thermal inertia, results in a temperature shift by 2-3 months with respect to the atmospheric seasonal cycle (Merlivat and Jouzel, 1979). This is a result of deuterium excess being a combined parameter of δD and $\delta^{18}\text{O}$, where each variable has different characteristics. Deuterium excess is correlated with air temperature, sea surface temperature, and humidity at the oceanic source area of the precipitation. δD and $\delta^{18}\text{O}$ represents the temperature of the point of condensation (at the cloud height). A consequence of this is that deuterium excess reflects a greater stability of the mid-latitude atmospheric circulation and hydrological cycle, whereas δD and $\delta^{18}\text{O}$ is a representation of the transport of heat and moisture toward the northern latitudes as described by Merlivat & Jouzel (1979).

Deuterium excess is a useful application caused by the difference in diffusion for δD and $\delta^{18}\text{O}$. The consequence of $\delta^{18}\text{O}$ diffusing with a higher velocity than δD as mentioned in chapter 2.1,

gives deuterium excess a variation that represents the seasonal variability before the diffusion gets too dominating (Johnsen et al., 1989).

Based on this, it should be possible to determine the annual cycle in the upper part of the firn core by looking at the deuterium excess graph - figure 4.2. If the curve has high amplitude and a clear period it can be regarded as 1 year, which is due to the difference in diffusion.

2.4 Precipitation

The density of each ice sample is a useful tool when examining the drill site. When looking at the firn zone (this ice core), the density is increasing with depth. This is a consequence of the firn getting compacted by the overlying layers and water vapour diffusion (Cuffey and Paterson, 2010). The density variation for this core is around $(250 - 650) \frac{\text{kg}}{\text{m}^3}$, and therefore the firn-ice transition zone is not reached ($830 \frac{\text{kg}}{\text{m}^3}$).

It is possible to determine the annual mean precipitation by combining the change in density with the knowledge about the specific year at a given depth. In other words, the age-depth correlation makes it possible to determine the amount of accumulated snow each year, and by combining this knowledge with the changing density through the depth, it is possible to substantiate the annual mean precipitation:

$$\text{Annual precipitation} \left[\frac{\text{cm}}{\text{y}} \right] = \text{layer thickness} \left[\frac{\text{cm}}{\text{y}} \right] \cdot \frac{\text{density of the layer} \left[\frac{\text{kg}}{\text{m}^3} \right]}{\text{density of glacier ice} \left[\frac{\text{kg}}{\text{m}^3} \right]}. \quad (2.8)$$

Glacier ice has a density of $917 \frac{\text{kg}}{\text{m}^3}$ (Cuffey and Paterson, 2010). The reason for multiplying the layer thickness for one year with the ratio of the density is to compensate for the ice being compressed. This estimation is however strongly affected by the dating of the core. For instance, if a year was marked wrong, the layer thickness will either be too high or too low. Thus, multiplying with the changing density ratio, the estimated precipitation will be incorrect, hereby resulting in a wrong approximation of the annual precipitation.

3 Experiment

3.1 Sampling the ice core

This experiment focuses on the upper 29 meters (28.60 meters) of the NEGIS firn core. The core has been transported to the Centre for Ice and Climate, Niels Bohr Institute, where it has been processed. First an analysis with the Electric Conductivity Method (ECM) was performed, with the purpose of measuring the conductivity of the core, which is valuable for detecting annual layers and detecting volcanic eruptions - this will not be described any further. During this project, the core was then cut to appropriate sizes depending on the method of analysis. The analysis of the stable isotopes required 5 cm samples - see figure 3.1. In this experiment every 5 cm is regarded as a discrete sample, thus, every 5 cm represent one isotopic composition. A smaller sample would probably not yield a better resolution, as a consequence of the low accumulation rate and high diffusion. This differs from the Continuous Flow Analysis (CFA) where the isotopic composition is measured continuously while melting the core. Comparing the measurements of the discrete samples and the CFA give a great insight into the variability of the isotopes in the core, and this can justify the chosen length of 5 cm.

The core consisted of an ice core divided in bag 3-52 (1.10 - 28.60 meters), and a separate snow piston core (0 - 1.50 meters), thus resulting in 583 samples. A bag is defined by the accurate

depth at which it was drilled and logged before being cut and subsampled, which is very useful when creating the depth scale. A snow piston consist of surface snow, and the snow was divided into three overlapping bags each consisting of a 55 cm core. The third snow piston (0.95 - 1.50 meters) overlapped with both the second snow piston (0.50 - 1.05 meters) and the first ice core bag (1.10 - 1.65 meters). It is essential to have in mind, that the data is overlapping, when analysing the isotopic composition. Particularly in the circumstance of the third snow piston, since it is overlapping with the ice core, some data has to be discarded.

The rest of the core was divided into bag 3-52, where each bag consisted of a 55 cm ice core. A consequence of the overlapping depth of the snow pistons was that the data had to be linked together, which was made possible by examining the isotopic composition. In other words, by looking at the isotopic pattern it is possible to see where the data overlap, and check if the values are equal and consistent across samples of the same depth, hereby making it possible to treat the overlapping data as one - see figure 4.1.



Figure 3.1: Here the 5 cm samples are getting cut and prepared for further measurements.

Hereafter, the samples have systematically been melted. The melting process is done after a method created by Willi Dansgaard. In relation to the theory, evaporation of the isotopes is unwanted. The melting was done by using dry airtight tobacco containers where the pieces of the ice core were placed. Afterwards, the melted ice was poured into small plastic containers, where the samples could be stored. These plastic containers were either being kept frozen or cold in the refrigerator and away from sun light to avoid evaporation.

A pipette was used to dispense 1.5 mL of every sample into 2 mL vials. When pipetting the samples, the tip of the pipette was changed for every sample to avoid water residues from contaminating between the samples.

3.2 IR cavity ringdown spectroscopy

3.2.1 Theory behind the spectroscopy

Water molecules have spectral absorption lines in the mid - and near infrared area because of its rotational and vibrational transitions (ro-vibrational transition). This is a result of the absorbed radiant energy, which lets the molecule oscillate around its equilibrium position (de Groot, 2004). If the corresponding sample pressure is low, then the absorption lines from the water molecules are narrow enough to differentiate between the different isotopologues (Gkinis et al., 2010).

The theory behind ringdown spectroscopy is that a laser is beaming through a cavity until a certain intensity threshold is reached. Hereafter, the laser is shut down and the beam will now start decaying. The time it takes for the beam to decay is called the ringdown time. In addition to that, if something that absorbs light (water vapour) is in the cavity, then the decay will happen

faster. Thus, it is then possible to determine the concentration of the various isotopologues by analysing the ringdown time. This task is the Picarro software set up to do.

This is the main theory behind infrared cavity ringdown spectroscopy (IR-CRDS)- for more details, see Gkinis et al. (2010).

The different isotopologues of the water molecules have different absorption bands in the near-infrared spectrum as a result of the difference in their ro-vibrational transitions (de Groot, 2004) as seen in figure 3.1. The wavelengths were measured with the Picarro L2120-i for an accurate and precise value, hereafter compared with Kerstel et al. (2006) to classify the precise isotopologue and the corresponding wavelength.

Isotopologues	H ¹⁸ OH	DOH	H ¹⁶ OH
Wavelength [nm]	1392.063	1391.987	1392.043

Table 3.1: The different absorption bands of different isotopologues in the near-infrared spectrum.

3.2.2 Procedure

The CRDS consists of a vaporiser box, a hot box where the cavity consisting of the mirrors are mounted, and a warm box consisting of a wavelength monitor chamber. First, a syringe taps a 15 μ L sample. Then it transfers the water to the vaporiser box, where it is injected [1] - see figure 3.2. The vaporiser box consists of a fused silica capillary, and during the pumping, the water is continuously vaporised with 100 % efficiency into a box with a temperature at 170 °C. If it's not evaporating with 100 % efficiency, then isotopic fractionation can occur, which would destroy the very signal this project is trying to detect from natural processes in this experiment.

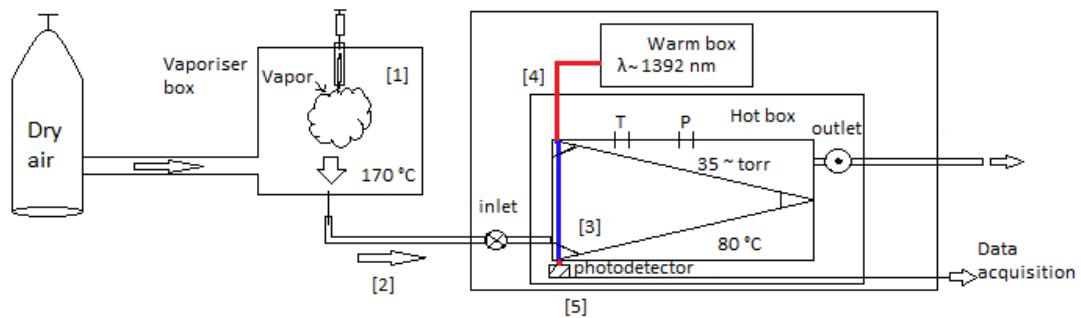


Figure 3.2: Experimental set-up showing how the sample is transferred from liquid to vapour state, and afterwards how the isotopic composition is measured. The numbers represent the order in which the CRDS analyses the water sample, which is specified in chapter 3.2.2. The blue line represents the laser beam, and the red line represents the optical fibres in which the laser travels. The circle with an x is the vapour inlet, and the circle with a dot is the gas outlet. The valves controlling the pressure are placed at the inlet and outlet. The T and P in the set-up illustrates that the pressure and temperature in the cavity have to be stable.

Here the gas is enclosed within the box which is filled with dry air. This mixing results in a gas sample with the desired water vapour level (settings are described further down). The dry air also serves as a carrier for the vaporised sample, hereby transporting it through an open-split

tube into a stainless tube with a flow rate of 30 mL/min. The idea behind the open-split configuration is that the pressure in the machine has to be around 1 atmosphere, which is automatically maintained by the open-split tube, as a result of the open-split letting out air if the pressure gets too high [2]. It is of great importance that the pressure and the temperature in the cavity are stable. Additionally, the pressure had to be low as mentioned earlier, which is maintained with 35 torr (≈ 46.67 mbar). The gas flow is regulated by two valves as seen in figure 3.2. A valve is placed where the gas enters the cavity (inlet), and the other one where the gas leaves the cavity (outlet). One of them will allow a constant flow, while the other one will vary with the purpose of keeping the pressure stable.

Furthermore is the temperature being kept stable by layers of surrounding material insulating the cavity, and a heat sink to redirect the heat if the cavity gets too warm. A precision around ± 20 m $^{\circ}$ C is hereby obtained.

The sample then arrives at the hot box (80 $^{\circ}$ C), which consists of three high-reflective (R) mirrors shaped like a V (R > 99.9 %) [3]. A wavelength monitor located in the warm box (45 $^{\circ}$ C) generates a wavelength with a value around $\lambda \approx 1392$ nm (see table 3.1), and the laser beam travels through optical fibres until it reaches the cavity [4] - red lines in figure 3.2. When the laser has reached the cavity it begins to build up the intensity until a certain threshold. When the threshold is reached it is abruptly shut down.

This results in an exponential decay of the light with respect to time (ringdown time) due to absorption and scattering as a result of the loss of light from the reflection by the mirrors - the blue line represents the laser in figure 3.2. Here the laser is beaming back and forth while the machine analyses the isotopic composition with an average path around 10 km (de Groot, 2004). The photo detector records the decreasing signal, and send the information to the data acquisition [5], hereby making it possible to determine the concentration of the different isotopes by analysing the absorption of the different wavelengths as seen in table 3.1.

The benefit of no laser light entering the cavity makes this technique almost immune to laser amplitude noise (de Groot, 2004). This results in an enhanced precision.

Every experiment consists of 3 standards and 39 discrete samples and took 7 hours to run. The CRDS has been programmed so that each standard is injected 12 times, and every water sample is injected 4 times. The reason for the 12 injections of the given standards are a result of the importance of having precise and accurate values of the standards free of memory effect. Furthermore, the difference in the δ -values for the three standards are relatively high, where the discrete samples have closer values. A more detailed description regarding the measurements will be given in chapter 4.

Another important feature is the addition of dry air. Previous experiments from Gkinis et al. (2010) has shown that data with the lowest standard deviation is found with a $\text{H}_2\text{O}_{conc}$ in the interval 17,000 - 22,000 ppmv (parts per million by volume). As a result of that, this experiment will be performed in the interval 19,000-20,500 ppmv. It is furthermore important to have each injection be as close to the others as possible (thus the narrow range of 19,000-20,500 ppmv). Typically, dry air will have a $\text{H}_2\text{O}_{conc}$ below 100 ppmv, which is quite insignificant to a measured value around 20,000 ppmv, so the systematic error of this method is relatively low.

4 Results

4.1 Data processing

The CRDS does not clean the syringe after each measurement, which allows traces of the previous water sample to contaminate the subsequent measurement. In order to minimize the contamination, the first 4 of 12 injections of each standard are discarded, and the first 1 of 4 injections for the given discrete sample is discarded as well. Thus, after respectively 1 and 4 injections are removed the equipment is as close as possible to being rid of traces from the previous water sample. Memory also comes from the cavity and the vaporiser, but the syringe is the only parameter, which is able to account for.

When the memory effect from the syringe has been taken into account, the average of the remaining data for each sample will now be calculated as a representation of the discrete sample. Hereafter, the data can now be calibrated.

4.2 Calibration

The CRDS calculates the demanded δ -values, but to make sure it represents the right isotopic composition of the ice core, it is of crucial importance to calibrate the data.

When calibrating the data 3 standards are being used. These standards are given by the International Atomic Energy Agency (IAEA), and its corresponding values are known. These standards are relative to Vienna Standard Mean Ocean Water (VSMOW). Therefore, by measuring them it is possible to estimate the accuracy of the spectrometer. This is done by plotting the exact values and the measured values on a graph. If it was calibrated correctly a linear curve where the slope is 1 should occur, and the curve should go through the point (0,0). However this is never the case, which enhances the importance of calibrating the data. The calibration is done with knowledge about the slope and the intercept on the y-axis (VSMOW), which gives the following equation:

$$\delta_{calibrated} = \text{slope} \cdot \delta_{measured} + \text{intercept}. \quad (4.1)$$

The standards relative to VSMOW, can be seen in table 4.1. Even though instrumental drift should be minimal it will be avoided by calibrating the data. Furthermore, each experiment finishes by measuring the NEEM standard again 4 times, which will make it possible to determine whether or not there has been an instrumental drift throughout the experiment.

Standards	$\delta^{18}\text{O}_{\text{VSMOW}}[\text{‰}]$	$\delta\text{D}_{\text{VSMOW}}[\text{‰}]$
- 22	- 21.89	- 168.7
NEEM	- 33.44	- 257.3
- 40	- 39.79	- 309.8

Table 4.1: Standards relative to VSMOW.

4.3 Error analysis

When the results are calibrated, it is now relevant to look into the standard deviations of the data. As mentioned earlier, 3 measurements of every sample are used. These samples should arrange themselves as a Gaussian distribution around a mean value. However, 3 data points are not a great representation of a Gaussian distribution. The manufacture Picarro and Gkinis et al. (2010) state that the precision of CRDS is above 0.1‰ for $\delta^{18}\text{O}$ and 0.5‰ for δD . If a discrete sample has a standard deviation higher than this, the corresponding noise is too high,

which would result in the given measurement being discarded. However, this was never the case, which is a result of the precision of the CRDS.

Another relevant uncertainty occurs when defining the time-scale. When dating the ice core, the uncertainty of the time-scale will increase with depth. This is a result of having a precise time when the core got drilled, hereafter, only the isotopic composition and impurities have the dating properties, and in respect to error propagation the uncertainty will increase with depth (Taylor, 1997). However, historical volcanic eruptions are clear indicators of a precise year as mentioned in chapter 2.2.2. Therefore, the uncertainty around the eruptions will be reduced (Steig, 2008). One thing with volcanic eruptions to be concerned about, is the time it takes from the acid fallout to travel to the icesheet on Greenland, but this is a minor problem. Based on this, it is possible to date the ice core with a precision of 1 year. This is influenced by the large amount of different parameters with seasonal properties making it possible to determine a precise year. A systematic error occurs when arranging the ice samples due to cutting noises, which might influence the isotopic signal. However, a sample size of 5 cm should decrease the effect of this systematic error, since the signal-to-noise ratio gets smaller.

4.4 Data

After the ice core has been dated down through depth, it's relevant to use this dating to create annual average isotopic values. The annual time series of NEGIS $\delta^{18}\text{O}$ is shown in figure 4.5 (green curve). The same is done for the deuterium excess, and the annual time series is plotted together with the sea surface temperature (SST) in figure 4.7 (green curve).

The selection of the snow piston data were done by plotting the changing isotopic composition with respect to depth.

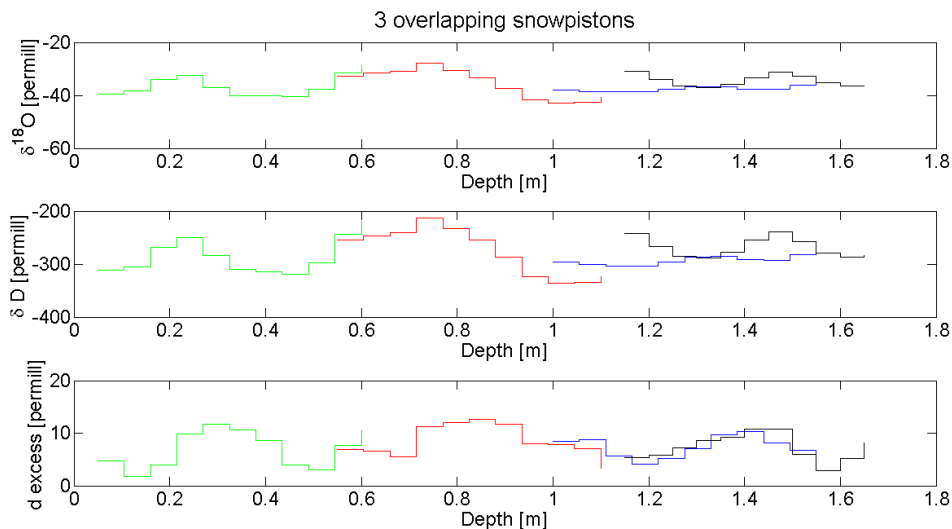


Figure 4.1: The three overlapping snow pistons and the beginning of the ice core (black curve) are here displayed. The first piston is green, the second is red and the third is blue.

The overlap between the first and second snow piston is not influencing any seasonal peak, and the two corresponding δ -values are almost identical, so linking that part is easy. Here the value from the second snow piston is chosen. The overlaps between the ice core and the two snow

pistons are however more difficult. When examining figure 4.1, the third snow piston reveals a very unclear amplitude compared with the ice core, where a more clear amplitude is given, and actually two seasonal cycles are here revealed. Normally, snow pistons have a larger uncertainty compared with ice cores as a consequence of the snow grains being able to move more freely. This results in larger fluctuations. Therefore, the third snow piston is discarded, which results in one missing data point of 5 cm. This will not change the overall results presented in this project.

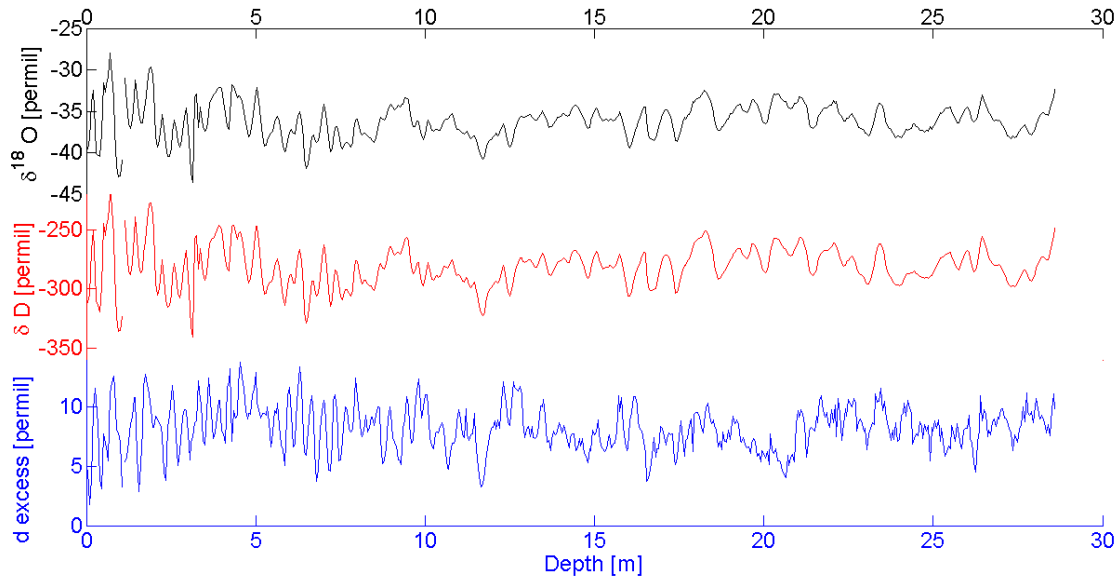


Figure 4.2: The stable isotope variation with changing depth presented as $\delta^{18}\text{O}$ (black curve), δD (red curve) and deuterium excess (blue curve). Deuterium excess is calculated via equation 2.6.

Stations	Upernavik	Danmarks- havn	Bjornoya	Jan Mayen	Tasiiliaq	Svalbard	SST
Latitude	72.8 N	76.8 N	74.5 N	70.9 N	65.4 N	78.1 N	0-70 N
Longitude	56.2 W	18.7 W	19.0 E	8.7 W	37.4 W	13.6 E	-
Years	1873-2011	1951-2012	1949-2012	1923-2012	1894-2011	1912-2012	1856-2012
Cor. ($\delta^{18}\text{O}$)	0.123	0.029	0.141	-0.141	0.189	-0.021	0.245
Sign. ($\delta^{18}\text{O}$)	35.2 %	17.7 %	73.7 %	81.7 %	95.6 %	16.8%	99.6 %
Cor. (excess)	-0.017	-0.159	-0.356	-0.108	-0.049	-0.083	-0.170
Sign. (excess)	14.8 %	78.9 %	99.6 %	69.3 %	39.9 %	59.1 %	95.2 %

Table 4.2: Coordinates for the coastal stations. The data from Tasiiliaq, Danmarkshavn and Upernavik is provided by (DMI) and the rest is given by (NASA). The correlation coefficient (Cor.) between each coastal station, $\delta^{18}\text{O}$, and the deuterium excess is given, and the corresponding level of significance (Sign.) is displayed (see figure 4.5).

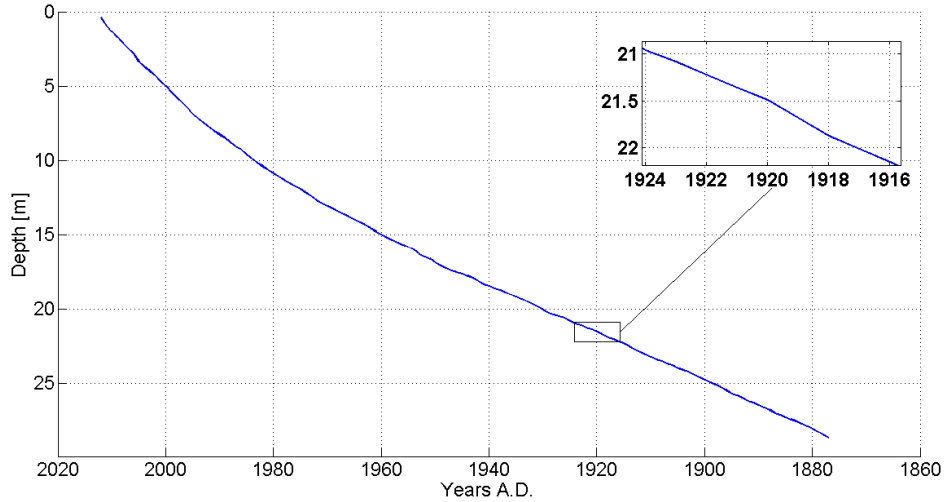


Figure 4.3: NEGIS depth-age relationship. The focus area is the depth interval in which the dating on figure 4.4 takes place.

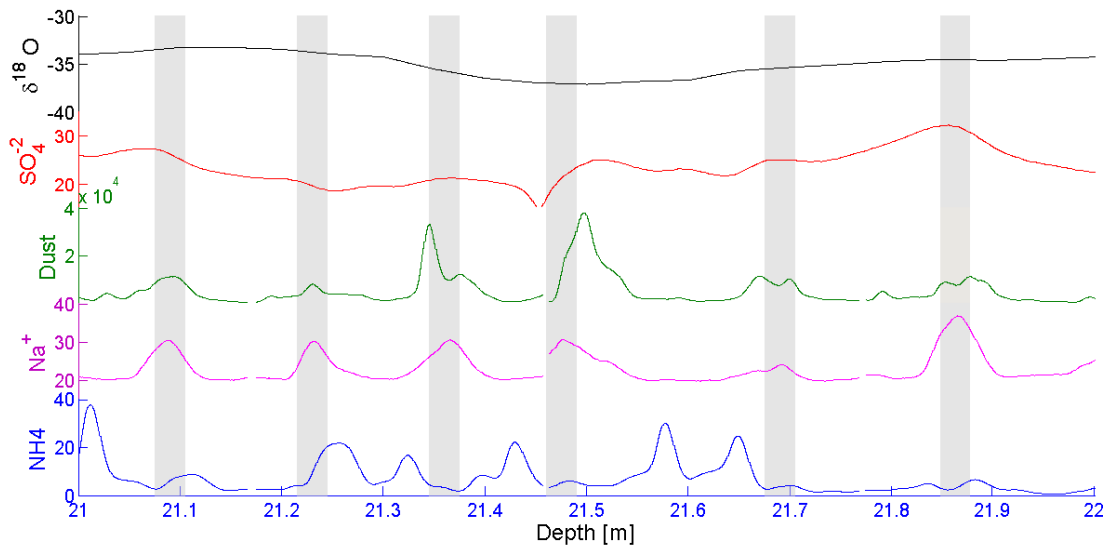


Figure 4.4: Dating of the core in the depth interval 21-22 meters. The grey rectangular boxes illustrate where a given year is marked based on the Na^+ (purple)- winter. A seasonal peak is confirmed by looking and verifying with the other seasonal dependent parameters such as Na^+ (purple), NH_4^+ (blue), SO_4^{2-} (red) and dust (green). The only parameter in this example which is not correlating with the others is NH_4^+ . The $\delta^{18}\text{O}$ (black) is here to diffused to reveal any annual variability. Units are not provided since it is the variations which are important.

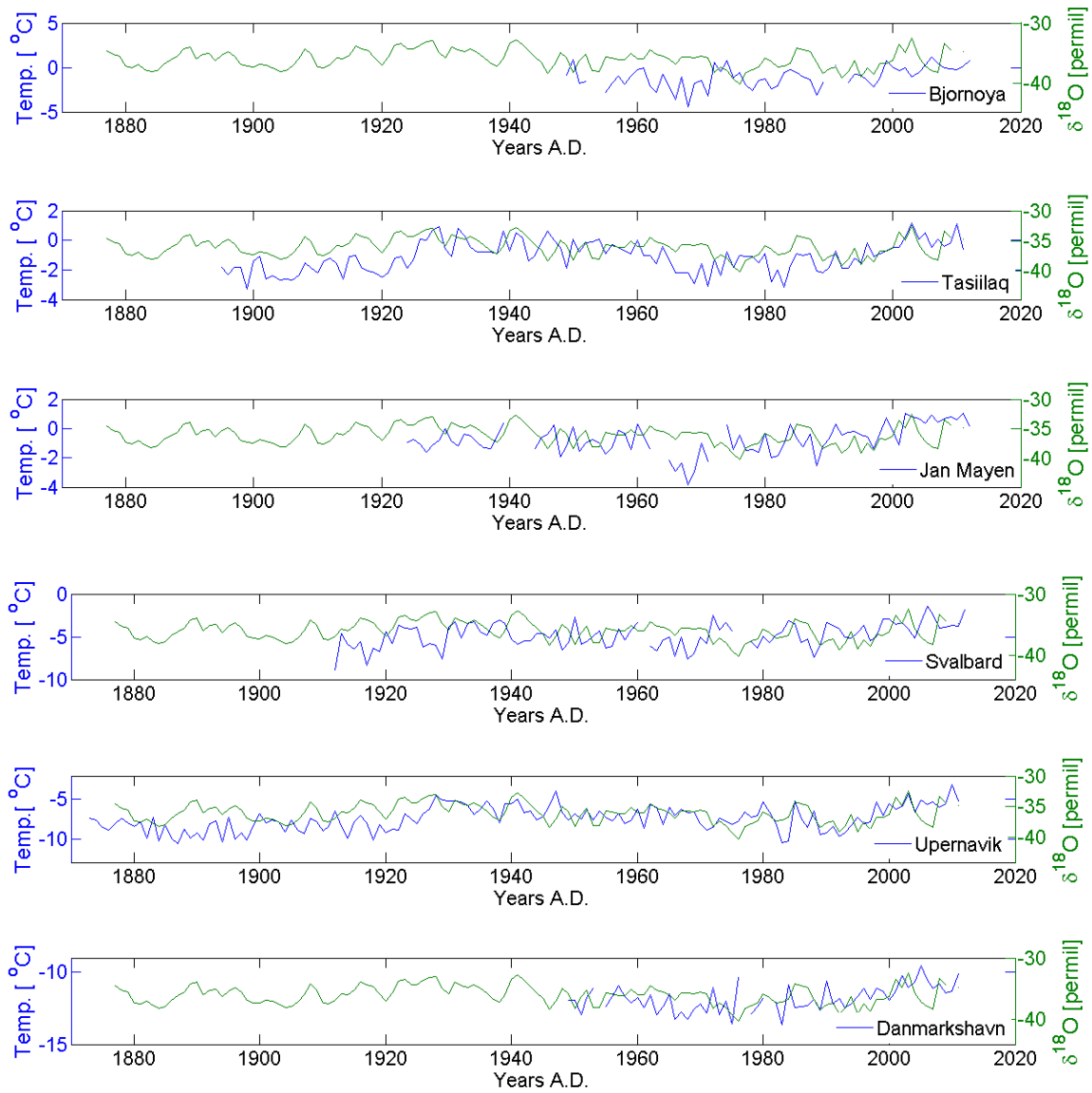


Figure 4.5: Here every coastal stations' temperature measurements (blue lines) and the $\delta^{18}\text{O}$ (green line) are plotted with respect to time. It is the same time interval for $\delta^{18}\text{O}$ in every plot. The gaps in the data are a result of missing measurements in that period. The coordinates and correlation coefficients are provided in table 4.2, and a map is provided in figure 2.1. The data from Tasiilaq, Danmarkshavn and Upernavik is provided by DMI and the rest is provided by NASA.

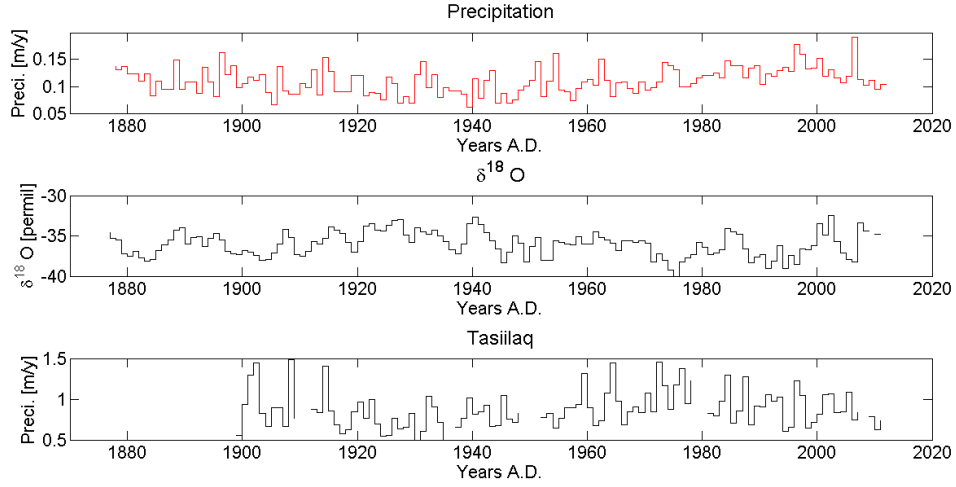


Figure 4.6: The upper red graph illustrates the calculated annual precipitation from the year 1877 till 2012 (see equation 2.8), and the black graph below shows the corresponding annual $\delta^{18}\text{O}$ with respect to time. The third plot shows the measured precipitation (1899-2011) from Tasiilaq provided by DMI. The annual precipitation from the first plot (red curve) in that time interval is estimated to $11 \pm 2 \frac{\text{cm}}{\text{y}}$. The gaps in the data are a result of no measurements due to labour strike etc.

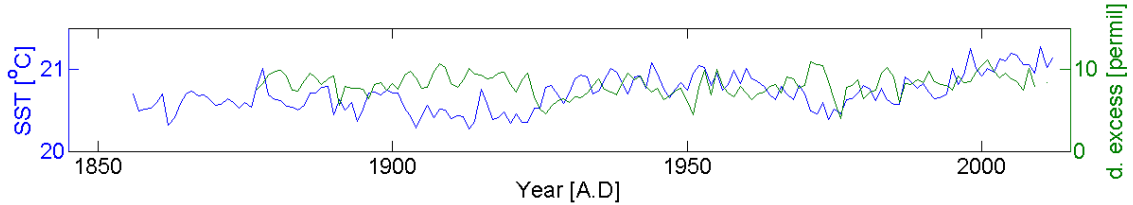


Figure 4.7: Relationship between the annual deuterium excess (green curve) and annual measured SST (blue curve) - Sea Surface Temperature. The deuterium excess is in the time interval 1877-2011 and the SST is from 1856-2012. The SST is provided by NOAA (2013).

5 Discussion

The third snow piston overlapped with the first ice core bag, as seen in figure 4.1, which resulted in the need to discard some data. The measured isotopic composition of the third snow piston revealed an unclear and noisy signal of the stable isotopes, whereas the results from the ice core (bag 3) had a more clear and undisturbed signal. On this, the third snow piston was chosen to be discarded which resulted in one missing data point (5 cm) at a depth of 1.05 - 1.10 meters.

The stable isotopes which were measured and calibrated are illustrated in figure 4.2. Here $\delta^{18}\text{O}$, δD and the deuterium excess are plotted as a function of depth. In addition, the deu-

terium excess has a clear amplitude and period in the upper 10 meters, whereas the amplitudes belonging to $\delta^{18}\text{O}$ and δD begin to fade after 7 meters. The difference between the diffusion velocities of $\delta^{18}\text{O}$ and δD result in a clear amplitude in deuterium excess, which figure 4.2 confirms. Deeper within the core, the period and amplitude begin to fade for all the parameters which is a consequence of the low accumulation rate. A low accumulation rate results in a thin annual layer thickness, which in turn results in a dominating diffusion. This is why the varying isotopic composition alone is not suitable for dating the ice core. Deconvolution of the data (i.e. calculating the back-diffusion) is not relevant since the seasonal variability of the $\delta^{18}\text{O}$ are too diffused to reveal anything. Therefore the focus will centre on annual variability.

Figure 4.5 consists of six plots, each displaying a measured coastal temperature record from a given station in the North Atlantic together with the measured $\delta^{18}\text{O}$ found in this project - coordinates are given in table 4.2. For every station the correlation between $\delta^{18}\text{O}$ and the measured temperature are calculated. Every coastal station has a different time interval, where the temperature was measured so only the measurements of $\delta^{18}\text{O}$ corresponding to the same time period were used.

The method used in this project is based on Pearson correlation. A correlation coefficient is in the interval of $[-1;1]$, where 1 is a positive (increasing) linear relationship (correlation), and -1 is the case of a perfect negative (decreasing) linear relationship (anti-correlation). Therefore, the closer the correlation coefficient is to either -1 or 1, the stronger is the correlation between the variables. Moreover, if the coefficient is 0 then the two variables are completely uncorrelated. The correlation coefficient defines how well the two variables match but the coefficient is difficult to interpret. Normally some labelling systems exist to roughly categorise the correlation coefficients:

- > 0.9 ; Very high correlation
- $0.68 - 0.90$; Strong or high correlations
- $0.36 - 0.67$; Modest or moderate correlation
- $0.20 - 0.36$; Low or weak correlation
- < 0.20 ; No or negligible correlation

This characterisation is given by Taylor (1990), hence the corresponding negative values are applicable for anti-correlation. The correlation coefficients between every station, $\delta^{18}\text{O}$ and the deuterium excess are given in table 4.2. The correlation coefficients regarding $\delta^{18}\text{O}$ are very low and can be classified as no or negligible correlation. The only station, which is close to being weakly correlated, is Tasiilaq with a coefficient of 0.189.

The coefficients for the correlations between the deuterium excess and the coastal stations are calculated as well. Here a low to modest anti-correlation of -0.356 between the measured temperature at Bjornoya and the deuterium excess are found. The deuterium excess is an indicator of the humidity and ocean temperature at the source of the precipitation. Consequently, this makes it difficult to state anything about the larger correlation with excess contrary $\delta^{18}\text{O}$. This is supported by Bjornoya being the only station anti-correlating with the deuterium excess, while also having a relative short time scale of 1949-2012.

However, a correlation between two variables can easily have a high or low correlation, but that does not justify whether or not the correlation only arises from random circumstances. In this project, the level of significance is calculated for every station displayed in table 4.2. The correlation coefficient is considered significant if the level of significance is above 95 %. When examining the results presented in this study, only Tasiilaq and Bjornoya have a significance level above 95 % (95.6 % and 99.6 %, respectively).

The correlation between $\delta^{18}\text{O}$ and the excess is estimated to -0.033, which is a negligible anti-correlation with a level of significance of 70.7% making it difficult to state any certain conclusion based on this. Although it is expected that $\delta^{18}\text{O}$ and excess anti-correlate since the excess

describes the temperature at the ocean source and humidity, whereas $\delta^{18}\text{O}$ describes the temperature at the condensation site, it is an insignificant anti-correlation. This might be a result of the low accumulation rate at the NEGIS site which consequently resulted in a dominating firn diffusion.

It is interesting that Tasiilaq has the highest correlation coefficient with $\delta^{18}\text{O}$ when Danmarkshavn, Jan Mayen and Bjornoya have shorter time scales. Normally, a shorter time scale should result in a higher chance of correlation. On the evidence, that was not the case for all the stations. However, concluding that no correlation exists at all between the measured $\delta^{18}\text{O}$ and measured temperature would be too quick a decision. On a closer inspection of the station Bjornoya at figure 4.5, the two graphs show a visible correlation in the 1980s till around 2000. The same is applicable for Danmarkshavn when making a visual examination. Here the temperature and $\delta^{18}\text{O}$ has a visible correlation with a small phase difference from the 1990s to around 2011. This small phase difference might be the reason why deuterium excess and Bjornoya has an anti-correlation of -0.356.

The small temperature variations for all the stations are different. This is because they all are located in different places around Greenland, some very far away from the NEGIS site as illustrated in figure 2.1. However a small tendency exists for the stations, since all the temperatures increase from around 1970 up until 2012 and afterwards increase through to around 1940. Hereafter, the stations Tasiilaq, Upernavik, and Svalbard illustrate a decreasing temperature. Figure 4.7 shows the area weighted average of the sea surface temperature (SST) from 0-70N over the North Atlantic provided by NOAA (2013) as well as the measured deuterium excess. The correlation coefficients between them are shown in table 4.2. The correlation coefficient of -0.170 and a level of significance of 95.2 % indicate only a negligible anti-correlation. However, $\delta^{18}\text{O}$ yields a correlation of 0.245 and a significance level of 99.6% which implies that a low correlation exists. The precipitation accumulated at NEGIS could originate in the whole area in which the SST averaged was taken. $\delta^{18}\text{O}$ has a higher correlation coefficient than deuterium excess with the measured SST which again might be a result of the low accumulation rate.

Stations	Upernavik Tasiilaq	Upernavik (+1) Tasiilaq	Tasiilaq (+1) Upernavik	Upernavik (+1) Upernavik	Tasiilaq (+1) Tasiilaq
Cor.	0.319	0.250	0.312	0.810	0.618
Sign.	99.9 %	99.3 %	99.6 %	> 99.9 %	> 99.9 %

Table 5.1: Here the correlation coefficients and level of significance are presented. The +1 is an indicator of shifting the data by 1 year, hereby simulating the consequence of an uncertainty in the dating of ± 1 year.

The dating of the core, which was essential in making the $\delta^{18}\text{O}$ s time dependency, has an uncertainty of ± 1 year. This is due to the great combination of different data as explained in chapter 2.2.2, which allowed a more precise interpretation of the various seasonal variations hereby making it possible to estimate a year with a high precision. However, the correlation coefficients of the temperature and $\delta^{18}\text{O}$ stated that almost no correlation existed between them. If a mistake was made in the dating of the core, then the annual $\delta^{18}\text{O}$ variation would probably have appeared differently. A mistake of 1 year may possibly have shifted the $\delta^{18}\text{O}$ and hereby changing the correlation coefficient. This is illustrated in table 5.1, where the coastal stations Tasiilaq and Upernavik have been examined for correlation. Here the correlation coefficients and level of significance are presented, and it is shown how large an effect the uncertainty of ± 1 year has on the correlation between the two coastal stations. If the correlation is calculated between Tasiilaq and Tasiilaq shifted 1 year, then the coefficient of correlation is reduced from 1 to 0.618. Tasiilaq and Upernavik has an correlation coefficient of 0.319 which decreases to 0.312 or 0.250, if either Tasiilaq or Upernavik is shifted by 1 year. This small example shows

how large an impact the uncertainty in the dating can have on the correlation.

A low correlation coefficient between $\delta^{18}\text{O}$ and measured temperature are not unusual, since a comparison only is made with one drill site. In Vinther et al. (2010), seasonal temperature correlations are found with the coastal station Stykkisholmur. Here some drill sites did not correlate with the measured temperature, although since 20 sites were presented an overall correlation existed. In White et al. (1997), correlations between the stable isotopes of snow and observed annual temperatures from coastal Greenland sites were presented as well. Equally, between some stations no correlation exists, however, when compared with a large number of other correlating drill sites an overall correlating appears to exist. Therefore, by comparing temperature measurements with only the NEGIS site, there is likely to be no correlation at all, especially as a consequence of the low accumulation rate.

The NEGIS ice core was drilled at an elevation of 2542 meters which would lower the temperature as a result of lapse-rate. Furthermore, $\delta^{18}\text{O}$ is only present by precipitation and is characterised by the temperature in the cloud and not at the accumulation site. Moreover, it is not possible to know if there has been an even monthly distribution of accumulated snow, which is an assumption in this project. The low accumulation rate results in a higher domination by sastrugi, a natural wind-driven process, causing the surface snow to undulate hereby arranging the annual accumulated snow unevenly. Another consequence of the low accumulation rate is the influence of sublimation. Sublimation is the transition from solid phase to vapour phase. This happens when the substance temperature and pressure are below the triple point in its phase diagram (Schroeder, 2004), presenting the possibility for snow to melt even though the temperature is below freezing point. In relation to the high elevation and recorded temperature at the closest coastal temperature station, Danmarkshavn (figure 4.5), the temperature should normally be below the freezing point, whereas ablation resulting in melting of snow should be non-existent. Furthermore, if the amount of accumulated snow at the site is low, then the effect of sublimation has a larger impact on the layer thickness. This combined with the dominating diffusion and sastrugi effects are a possible reason for the relationship between $\delta^{18}\text{O}$ and the temperature being far from ideal.

An annual mean precipitation was estimated to approximately $11 \pm 2 \frac{\text{cm}}{\text{y}}$ (1877-2012). The standard deviation approximated to $\pm 2 \frac{\text{cm}}{\text{y}}$ is an indicator of the variability from year to year. It is not expected that the precipitation would be identical each year. The precipitation and $\delta^{18}\text{O}$ at the site are illustrated in figure 4.6. Accordingly, the calculated annual precipitation variation is not consistent with the variation of $\delta^{18}\text{O}$. It was expected that a high $\delta^{18}\text{O}$ -value would be a representation of a large amount of precipitation, as a consequence of $\delta^{18}\text{O}$ being tantamount to a higher temperature and therefore accumulated snow. The inconsistency may be a result of glacial movement, since the core was drilled at the NEGIS site. The ice is moving 100 meters a year at NEGIS (personal correspondence with Christianson). The NEGIS site is effected by an upstream of $100 \frac{\text{m}}{\text{y}}$ of ice. As a result of that, the calculated precipitation in the 1940s might be the precipitation accumulated 7 kilometres further south. Furthermore is the site affected by topographic undulations, which affect the calculated precipitation (Christianson).

Figure 4.6 shows the measured precipitation from Tasiilaq. The correlation coefficient between the calculated precipitation and the measured precipitation at Tasiilaq is -0.237 with a level of significance of 98.9 %. These results indicate that a weak anti-correlation between them exists. However, it is difficult to offer anything conclusive based on this as a result of the upstream effect.

Further optimization of this study would include calculations of correlations coefficients in different time periods such as the last 20 years etc. This makes it possible to analyse if the coastal stations and $\delta^{18}\text{O}$ get very uncorrelated at a certain age, because a visual examination of the

correlations shown in figure 4.5 reveals a small tendency in the variations of the two variables.

6 Conclusion

The isotopic composition with support from seasonal varying parameters such as Na^+ , NH_4^+ , SO_4^{2-} and dust have made it possible to determine the depth with respect to time with a precision of ± 1 year. A consequence of the high diffusion due to the low accumulation rate resulted in a faded annual signal for $\delta^{18}\text{O}$ and δD after 7 meters as well as the deuterium excess after 10 meters, as seen in figure 4.2.

The annual isotopic composition of the NEGIS ice core has been determined in relation to the year of precipitation, and $\delta^{18}\text{O}$ was plotted separately with six different coastal stations temperature measurements as seen in figure 4.5. Furthermore, the excess was plotted together with SST in the North Atlantic - figure 4.7. Hereafter, the correlation coefficients and level of significance were calculated, which revealed Tasiilaq had the highest correlation coefficient of 0.189 with $\delta^{18}\text{O}$ and a level of significance over 95%. Additionally, Bjornoya had a weak anti-correlation of -0.356 with the excess and a level of significance of 99.6 %. However, none of the other stations had a correlation coefficient with $\delta^{18}\text{O}$ above the results from Tasiilaq. It has therefore not been possible to find any annual correlation between the coastal temperature data and the isotopic composition from the NEGIS core. This study found that the SST anti-correlated with the deuterium excess (-0.170) and correlated with $\delta^{18}\text{O}$ (0.245). All this is likely a result of the low accumulation rate, high elevation, affect of ± 1 year precision in the dating, sastrugi and the distance between the NEGIS site and the coastal stations.

Based on the age of the core, the varying layer thicknesses were calculated, which made it possible to estimate an annual mean precipitation around $11 \pm 2 \frac{\text{cm}}{\text{y}}$ (1877-2012). The changing precipitation over time was illustrated in figure 4.6, which reveals that inconsistency of $\delta^{18}\text{O}$ and calculated precipitation exist due to topographic undulations and an upstream of $100 \frac{\text{m}}{\text{y}}$. The measured precipitation at Tasiilaq was compared with the estimated precipitation at NEGIS, which revealed a correlation coefficient of -0.237 and a level of significance of 98.9 %. Therefore, a weak anti-correlation was present between the measured precipitation at Tasiilaq and the $\delta^{18}\text{O}$ from NEGIS. Likely, this low correlation is the same reason for the temperature data showing no correlation with the $\delta^{18}\text{O}$.

Bibliography

- J. Cappelen. *Greenland: DMI Historical Climate Data Collection 1873-2011*, volume 12-04. 2012. <http://www.dmi.dk/dmi/index/viden/dmi-publikationer/tekniskerapporter.htm>.
- Knut Christianson. PhD, Personal correspondence. 2013.
- H. Craig. Isotopic variations in meteoric water. *Science*, Vol. 133, no. 3465, pp. 1702-1703, 1961.
- K. M. Cuffey and W. S. B. Paterson. *The Physics of Glaciers*. Elsevier, 4th edition, 2010.
- Pier A. de Groot. *Handbook of Stable Isotope Analytical Techniques*. Elsevier, 2004.
- NOAA. Physical Science Division. URL <http://www.esrl.noaa.gov/psd/data/timeseries/AM0/>. Online; accessed 02-June-2013.
- Gibson J. J. Froehlich, K. and P. Aggarwal. *Deuterium Excess in Precipitation and its Climatological Significance*. Journal of Geophysical Research - Atmospheres, 2002.
- V. Gkinis, T.J. Popp, S.J. Johnsen, and T. Blunier. *A continuous stream flash evaporator for the calibration of an IR cavity ring-down spectrometer for the isotopic analysis of water*. Center for Ice and Climate, Niels Bohr Institute, University of Copenhagen, 2010.
- D.J. Griffiths. *Introduction to Quantum Mechanics*. Pearson Prentice Hall, 2th edition, 2004.
- Mook W.G. Grootes, P.M. and J.C. Vogel. *Isotopic fractionation between Gaseous and Condensed Carbon dioxide*. Z. Physik 221, 257-273 (1969), 1968.
- K.F. Herzfeld and E. Teller. *The Vapor Pressure of Isotopes*. Physical Review, vol. 54., 1938.
- S. J. Johnsen, J. W. C. White, and W. Dansgaard. The origin of arctic precipitation under present and glacial conditions. *Tellus B*, Vol: 41, No 4, 1989.
- E.R.T. Kerstel, R.Q. Iannone, M. Chenevier, S. Kassi, J.H. Jost, and D. Romanini. A water isotope (^2H , ^{17}O , and ^{18}O) spectrometer based on optical feedback cavity-enhanced absorption for in situ airborne applications. *Applied Physics B - Lasers and Optics*, 85, 397-406, 2006.
- L. Merlivat and J. Jouzel. *Global Climate Interpretation of the Deuterium-Oxygen 18 Relationship for Precipitation*. Journal of Geophysical Research, vol. 84, no. C8, 1979.
- J. Mook. *Environmental Isotopes in the Hydrological Cycle Principles and Applications*. International Atomic Energy Agency, 2000.
- NASA. Goddard institute for space and studies. URL http://data.giss.nasa.gov/gistemp/station_data/. Online; accessed 19-April-2013.
- S. O. Rasmussen. *Improvement, dating, and analysis of Greenland ice core stratigraphies*. PhD thesis, Niels Bohr Institute, University of Copenhagen, 2006a.
- S. O. Rasmussen. *Improvement, dating, and analysis of Greenland ice core stratigraphies*. PhD thesis, Niels Bohr Institute, University of Copenhagen, 2006b.
- S.O. Rasmussen, K.K. Andersen, A.M. Svensson, B.M. Steffensen, and B.M. Vinther. A new greenland ice core chronology for the last glacial termination. *Journal of Geophysical Research*, 111, 2006.
- D.V. Schroeder. *An Introduction to Thermal Physics*. Addison Wesley Longman, 1th edition, 2004.

- E.J. Steig. Sources of uncertainty in ice core data. *Contribution to workshop on: Reducing and Representing Uncertainties in High-Resolution Proxy Data*, 2008.
- J. Taylor. *An introduction to Error Analysis*. University Science Press, 1997.
- R. Taylor. Interpretation of the correlation coefficient: A basic review. *JDMS*, 1: 35-39, 1990.
- B.M Vinther, P.D. Jones, K.R. Briffa, H.B. Clausen, K.K. Andersen, D. Dahl-Jensen, and S.J. Johnsen. Climatic signals in multiple highly resolved stable isotope records from greenland. *Elsevier: Quaternary Science Reviews*, 29, 522-538, 2010.
- J.M. Wallace and P.V. Hobbs. *Atmospheric Science: An Introductory Survey*. Academic Press, 2th edition, 2006.
- J. W. C. White, L. K. Barlow, D. Fisher, P. Grootes, J. Jouzel, S. J. Johnsen, M. Stuiver, and H. Clausen. The climate signal in the stable isotopes of snow from summit, greenland: Results of comparisons with modern observations. *Geophys. Res. Lett.*, vol.: 102, C12, 26,425-26439, 1997.
- W. Dansgaard. *Stable isotopes in precipitation*. Tellus B, Vol: 16, Issue 4, pages: 436-468, 1964.
- W. Dansgaard. *The O^{18} -abundance in fresh water*. Geochimica et Cosmochimica Acta, Volume 6, Issues 5-6, Pages 241-260, 1964.